Published in final edited form as:
J Alzheimers Dis. 2013 January 1; 33(2): 407–422. doi:10.3233/JAD-2012-121438.

3xTg-AD Mice Exhibit an Activated Central Stress Axis during Early-Stage Pathology

Elaine K. Hebda-Bauer[a], **Tracy A. Simmons**[a], **Andrew Sugg**[a], **Eren Ural**[a], **James A. Stewart**[a], **James L. Beals**[a], **Qiang Wei**[a], **Stanley J. Watson**[a], and **Huda Akil**[a]
[a]University of Michigan, Ann Arbor, Michigan 48109

Abstract

Activation of the hypothalamic-pituitary-adrenal (HPA) axis occurs in response to the organism's innate need for homeostasis. The glucocorticoids (GCs) that are released into the circulation upon acute activation of the HPA axis perform stress-adaptive functions and provide negative feedback to turn off the HPA axis, but can be detrimental when in excess. Long-term activation of the HPA axis (such as with chronic stress) enhances susceptibility to neuronal dysfunction and death, and increases vulnerability to Alzheimer's disease (AD). However, little is known how components of the HPA axis, upstream of GCs, impact vulnerability to AD. This study examined basal gene expression of stress-related molecules in brains of 3xTg-AD mice during early-stage pathology. Basal glucocorticoid levels and mRNA expression of the glucocorticoid receptor (GR), mineralocorticoid receptor (MR), and corticotropic releasing hormone (CRH) in several stress- and emotionality-related brain regions were measured in 3–4-month-old 3xTg-AD mice. Despite normal glucocorticoid levels, young 3xTg-AD mice exhibit an activated central HPA axis, with altered mRNA levels of MR and GR in the hippocampus, GR and CRH in the paraventricular nucleus of the hypothalamus, GR and CRH in the central nucleus of the amygdala, and CRH in the bed nucleus of the stria terminalis. This HPA axis activation is present during early-stage neuropathology when 3xTg-AD mice show mild behavioral changes, suggesting an ongoing neuroendocrine regulation that precedes the onset of severe AD-like pathology and behavioral deficits.

Keywords

HPA axis; stress; corticotropic releasing hormone; glucocorticoid receptor; mineralocorticoid receptor; Alzheimer's disease

INTRODUCTION

Long-term activation of the hypothalamic-pituitary-adrenal (HPA) axis (such as with chronic stress) enhances susceptibility to neuronal dysfunction and death [for review see 1], thereby increasing vulnerability to neurodegenerative diseases such as Alzheimer's disease (AD). AD, the most common form of dementia and cognitive decline, is a devastating illness affecting 5.3 million Americans, with one in eight people over the age of 65 having the disease [2]. Since the onset of neuropathological changes precedes the appearance of cognitive deficits by many years [3, 4], treatments to slow or stop the progression of AD and preserve brain function will likely be most effective when administered early in the course

CORRESPONDENCE ADDRESS: Elaine K. Hebda-Bauer, PhD, Molecular & Behavioral Neuroscience Institute, University of Michigan, 205 Zina Pitcher Place, Ann Arbor, MI 48109, 734-936-2019 (office), 734-763-3771 (lab), 734-647-4130 (fax), hebda@umich.edu.

of the disease. Thus, the identification of risk factors that increase vulnerability to neurodegenerative disorders is critical for the development of prevention strategies.

One such potential risk factor is stress. Exposure to psychological and physical stressors is a universal phenomenon; but the manner with which an individual copes with stress varies considerably. Such differences in stress reactivity depend upon one's genetic predispositions and experiential responses and can increase one's vulnerability to neuropsychiatric and neurodegenerative disorders [5, 6]. Stress leads to activation of the HPA axis (to achieve homeostasis) resulting in the rapid synthesis and release of glucocorticoids (GCs) from the adrenal cortex into the circulation that then coordinate neural, immune, and endocrine responses to the stressor. The release of GCs from the adrenal cortex is stimulated by circulating adrenocorticotropic hormone (ACTH) released from the anterior pituitary. Upstream, ACTH release is triggered mainly by corticotrophin releasing hormone (CRH), which is synthesized and released by neurons in the paraventricular nucleus of the hypothalamus (PVN). The actions of GCs are mediated by two ligand-dependent transcription factors, the mineralocorticoid receptor (MR) and the glucocorticoid receptor (GR). MR is considered a regulator of the basal, diurnal tone of the HPA axis [7], while GR is considered a sensor of stress and a key player in the negative feedback limiting the stress response once it has taken place [8, 9, 10]. Considerable evidence indicates that HPA axis reactivity to stress is regulated by a number of limbic forebrain regions, including the hippocampus (HPC), amygdala, and prefrontal cortex [see 11 for review]. Having little direct input to the PVN, these limbic regions likely modulate CRH release from the PVN through a synaptic relay called the bed nucleus of the stria terminalis (BST) [12–14]. The HPC, rich in both MR and GR and playing a significant role in sending negative feedback to the PVN to turn off the stress response [11, 12], is a key brain structure involved in learning and memory and develops substantial AD neuropathology that begins very early in the disease process [3, 4]. The BST, in addition to being a major relay between the HPC and the PVN, is also considered part of the extended amygdala (including the central nucleus of the amygdala—CeA) because it plays a role in emotional behavior [15, 16].

Evidence from human and rodent studies point to chronic stress or exposure to excess GCs as increasing vulnerability to AD or accelerating cognitive and neural decline. Individuals who are more vulnerable to the adverse consequences of stress and exhibit higher levels of anxiety have an increased risk of AD and more rapid decline in global cognition [17]. Identifying such individuals may best serve as a marker for increased vulnerability to developing AD with an accelerated rate of cognitive decline, because these behaviors are not related to the continued progression of the common neuropathological markers (i.e., amyloid β (Aβ) plaques and tau neurofibrillary tangles) of the disease [18]. As early as middle-age, frequent or constant stress is also positively associated with the development of dementia, especially AD [19]. Among elderly individuals, those with dementia are less likely to exhibit cortisol (an endogenous GC) suppression after a dexamethasone (a synthetic GC) challenge [20, 21]. Baseline levels of GCs may not be different from young, but a delay in the turn off of the HPA axis (i.e., delay in the return of GCs back to baseline) in response to an acute stressor is the most commonly reported finding [22–24].

Recent evidence from animal models of AD shows that chronic stress or exposure to GCs exacerbates cognitive impairments [25–31] and enhances the accumulation of Aβor tau pathology [25, 27, 29, 32–34]. In the normal non-AD rodent brain, exposure to chronic stress or GCs has also been shown to shift APP processing to higher levels of β-secretase cleavage thereby producing more Aβ [26] or to increase tau phosphorylation [35]. Further, excess GC exposure via injections has been shown to increase Aβ levels and tau pathology in AD transgenic mice with early-stage pathology, particularly influencing intraneuronal Aβ accumulation in the HPC before any plaque pathology develops [33]. The association of

chronic stress or excess GC exposure with early cognitive impairment and exacerbated neuropathology in humans and animal models suggests that other, more central, elements of the HPA axis might be altered and such alterations may precede substantial Aβ accumulation and tau changes, serving as a risk factor for AD. Little is known about the extent to which stress-related molecules involved at other levels of the HPA axis (apart from GCs) are involved in modifying vulnerability to AD. Thus, the purpose of our study is to examine gene expression of stress-related molecules (GR, MR, and CRH) in brain regions known to exert control over the HPA axis and emotionality and anxiety-like behavior during early-stage pathology in the 3xTg-AD mouse model of Alzheimer's disease.

MATERIALS AND METHODS

Animals

Wild type (WT) and homozygous triple transgenic AD (3xTg-AD) mice possessing PS1M146V, APPswe, and tauP301L transgenes [36] were generated from breeding pairs kindly provided by Frank LaFerla (UC Irvine) from the colony at the Jackson Laboratory. Mice were housed on a 14:10 light/dark cycle (lights on at 6:00 A.M.) with *ad libitum* access to food and water. Genotypes were determined by PCR from tail DNA. Males and females were used because of the recently reported gender differences in neuropathology and behavior in this transgenic line [37–40]. All procedures were conducted in accordance with the guidelines outlined in the National Institutes of Health Guide for the Care and Use of Animals and were approved by the University Committee for the Use and Care of Animals at the University of Michigan.

Behavioral Testing

Since increased emotionality and other behavioral and psychological symptoms of dementia (BPSD) often precede cognitive impairment in humans [41], we assessed emotionality and anxiety-like behavior in young 3xTg-AD mice. Six-month-old male and female WT and 3xTg-AD mice (N=7–8 per group; 30 total mice) were tested in the elevated plus maze (EPM) and open field. A videotracking system (Ethovision, Noldus Technology) was used to collect behavioral data during these tests. The EPM consists of four arms (27 × 6 cm) arranged in a plus form and elevated 51 cm from the floor. Two opposing arms are surrounded with 14-cm-high clear Plexiglas walls (closed arms), whereas the other arms are devoid of walls (open arms). At the intersection of the four arms is a central 8 × 8 cm square platform giving access to all arms. Mice were gently placed in the center area and their behavior monitored for five minutes. The light intensity in the open arms was 275 lux. An entry is defined as a mouse having all four paws in an arm. Dependent measures included the time spent and number of entries into the open and closed arms and the center area and the distance traveled in the whole maze.

The open field is 72 cm^2 with walls 35.5 cm high and made of white acrylic. The light intensity in the center of the open field was 325 lux. Mice were placed in the center of the open field and their behavior monitored for five minutes. Dependent measures included the distance traveled, the latency to enter the periphery, the time spent in the center (36 cm^2), and velocity. Other measures of emotionality in the EPM and open field tests included the latency to move after being placed in the apparatus and the number of defecation boli generated during each five-minute test.

Corticosterone Radioimmunoassay

To determine basal glucocorticoid (i.e., corticosterone) levels, blood was collected from 3–4-and six-month-old female and male WT and homozygous 3xTg-AD mice (N=7–9 per group; 63 total mice) within 2 minutes after removal from their cages between 7:00 and

10:00 A.M. Blood was centrifuged within one hour of collection and plasma stored at −80°C until assayed. Plasma corticosterone (CORT) was measured using a commercially available radioimmunoassay kit (MP Biomedicals, Orangeburg, NY) according to package instructions. The sensitivity of the CORT radioimmunoassay was 0.77 μg/dl and the intra- and inter-assay coefficients of variation were less than 10%.

GR, MR, and CRH *In Situ* Hybridization Histochemistry

Since stress may serve as a risk factor for AD, we sought to determine the state of the hypothalamic-pituitary-adrenal (HPA) axis early in the disease process. Given that we observed mild altered emotionality in six-month-old 3xTg-AD mice, we chose an earlier age (3–4-months) to obtain brains from male and female WT and homozygous 3xTg-AD mice (N=7–9 per group; 33 total mice) for *in situ* hybridization histochemistry of stress-related molecules. This age was also chosen because it represents early-stage AD pathology in this animal model in which some hAβPP/Aβ and very little tau are detected in the hippocampus (limited to the pyramidal cell layer), cortex, and basolateral amygdala, and no plaques are present [42]. This age is also prior to the time at which consistent cognitive, emotional, and anxiety-like behavioral alterations are observed [37, 43]. Mice were sacrificed by rapid decapitation, and their brains removed, snap frozen, and stored at −80°C. Brains were cryostat sectioned at 10 μm, and sections were mounted on Fisherbrand Superfrost/Plus Microscope Slides. Sections were processed for *in situ* hybridization as follows. Sections were fixed in 4% paraformaldehyde at room temperature for 1 h. The slides were then washed three times in room temperature 2x SSC (300 mM NaCl/30 mM sodium citrate, pH 7.2), 1 min each wash. Next, the slides were placed in a solution containing acetic anhydride (0.25%) in triethanolamine (0.1 M), pH 8.0, for 10 min at room temperature, rinsed in distilled water, and dehydrated through graded ethanol washes (50%, 75%, 85%, 95%, and 100%). After air-drying, the sections were hybridized with a ^{35}S-labeled cRNA probe for MR, GR, or CRH. The GR probe is a 597-bp fragment directed against the mouse GR mRNA coding sequence. The MR probe is a 281-bp fragment directed against the mouse MR mRNA. The CRH probe is a 571-bp fragment directed against the mouse CRH mRNA. All cRNA probes were synthesized in our laboratory. The probes were labeled in a reaction mixture consisting of 1 μg of linearized plasmid, 1x transcription buffer (Roche, Indianapolis, IN), 120 μCi of ^{35}S-labeled-UTP, 125 μCi of ^{35}S-ATP, 400 μM CTP and GTP, 10 mM dithiothreitol, 4 units of RNase inhibitor, and 20 units of T7 (for MR and CRH) or T3 (for GR) RNA polymerase. The reactions were incubated for 90 min at 37°C, and then 10 units of DNase I (RNase free) was added to the reaction to incubate for another 15 min at room temperature. The labeled probes were purified using Micro Bio-Spin 6 Chromotagraphy Columns (Bio-Rad Laboratories, Hercules, CA), then diluted in hybridization buffer (containing 50% formamide, 10% dextran sulfate, 3x SSC, 50 mM sodium phosphate buffer, pH 7.4, 1x Denhardt's solution, 0.2 mg/ml yeast tRNA, and 20 mM dithiothreitol) to yield 2×10^6 dpm/80 μl. A coverslip with 80 μl of diluted riboprobe was placed on each slide. Slides were placed in a humidified box with filter paper saturated with 50% formamide buffer, and incubated overnight at 55°C. Following hybridization, coverslips were removed and the slides were washed in room temperature 2x SSC three times for 1 min each, and then incubated for 1 h in RNase A (200 μg/ml in 8.8 mM Tris-HCl buffer containing 0.5 M NaCl, pH 8.0) at 37°C. The slides were then washed in increasingly stringent SSC solutions: 2x, 1x, and 0.5x for 1 min each at room temperature, followed by incubation for 1 h in 0.1x SSC at 65°C. Finally, slides were rinsed in distilled water and dehydrated through graded ethanol washes, air-dried, and placed in autoradiography cassettes with Kodak XAR film (Eastman Kodak, Rochester, NY) placed on top for 4 (MR), 10 (GR) or 30 (CRH) days. The specificity of hybridization was confirmed by control experiments using sense probes or tissue that had been pretreated with

RNase A (200 μg/ml) for 1 hr at 37°C before hybridization with antisense probes. No specific hybridization signals were observed in these conditions.

Autoradiograms were digitized using a ScanMaker 1000XL Pro (Microtek, Carson, CA) with LaserSoft Imaging software (AG, Kiel, Germany). Digitized images were analyzed using Image J (NIH) at the rate of 63 pixels/mm. Optical density measurements were taken from the left and right sides of the brain at 70 μm intervals (1 in 7 series) throughout the rostro-caudal extent of each region of interest. Thus, for each animal, an average of 14–17 sections were analyzed from four subregions of the dorsal HPC (Cornu Ammonis fields CA1–CA3, and the dentate gyrus) for MR and GR, 5–6 sections from the PVN for GR and CRH, 18–20 sections from the central nucleus of the amygdala (CeA) for GR and CRH, and 5–6 sections from the BST for CRH. Optical density measurements were corrected for background (i.e., tissue area without signal) on each brain slice. Signal pixels of a region of interest were defined as being 3.5 standard deviations above the mean of the background. The average signal for a given measurement was then multiplied by the area sampled to produce an integrated density measurement. These data were averaged to produce one data point for each region per animal, and then group averages were calculated and compared statistically. Since a pre-specified area of the dorsolateral BST (BSTLD), and not the whole nucleus, was used to obtain optical density measurements, the BSTLD data are reported as the average signal intensity.

hAβPP/Aβ Immunohistochemistry

To verify early-stage Alzheimer's-like neuropathology in the 3–4-month-old 3xTg-AD mice, sections adjacent to those used for *in situ* hybridization histochemistry (N=9 males, 7 females; 16 total mice) were processed simultaneously for immunohistochemistry using the well-characterized 6E10 anti-hAβPP/Aβ antibody (Covance). Using this antibody allowed us to assess the presence of uncleaved APP, soluble APP cleaved at the alpha site (sAPPalpha), and Aβ (epitope: 3–8). Sections were fixed in 4% paraformaldehyde at room temperature for 1 h. The slides were then washed three times in room temperature PBS (0.02 M KPO_4, 0.16 M NaCl), 1 min each wash. Next, the sections were incubated in 50% formamide/2x SSC (300 mM NaCl/30 mM sodium citrate, pH 7.2) at 65°C for 2 h, rinsed 2 times in 2x SSC, then incubated in 2N HCl at 37°C for 30 min, followed by incubation in 100 mM sodium borate, pH 8.5, at room temperature for 10 min. Following 3 more rinses (1 min each) in PBS, the sections were incubated in 0.1% H_2O_2 to quench endogenous peroxidase activity. Next, the sections were rinsed 3 times in PBS, incubated with Avidin blocker (1:5 dilution, Vector Laboratories) at room temperature on a shaker for 15 min, rinsed 3 times in PBS, and then incubated with Biotin blocker (1:5 dilution, Vector Laboratories) at room temperature on a shaker for 15 min. Following 3 more rinses in PBS, sections were then incubated with BSA diluent (150 mM NaCl, 34 mM K_2HPO_4, 17 mM KH_2PO_4, 1% BSA, 1% NGS, 0.4% Triton) at room temperature for 1 h. Next, the 6E10 primary antibody was applied at a dilution of 1:5,000 and incubated at room temperature overnight. The next day, sections were rinsed 3 times in PBS and then incubated with a biotinylated goat anti-mouse secondary antibody (diluted 1:1,000; Vector Laboratories, Inc) at room temperature for 1 h. Sections were then rinsed 3 times in PBS and incubated in VECTASTAIN Elite ABC reagent (Vector Laboratories) diluted 1:1,000 in BSA diluent at room temperature for 60 min. The sections were then rinsed 2 times in 0.1 M sodium acetate (1 min washes) and then incubated in diaminobenzidine (1 mM diaminobenzidine, 105 mM $NiCl_2$, 0.006% H_20_2 in 0.1 M sodium acetate) at room temperature on a shaker for 6 min. The reaction was stopped by rinsing 3 times (1 min each) in distilled water. The sections were then dehydrated through graded ethanol washes (1 min per alcohol: 50%, 70%, 80%, 95%, 100%) and Xylene and coverslipped. A blocking peptide for 6E10 (RPEP-579P, Covance) completely blocked the immunoreactivity of the 6E10 antibody; thereby,

demonstrating the specificity of the antibody. Sections from WT mice also did not show any immunoreactivity for the antibody.

Images of the posterior parietal association cortex, CA1 area of the HPC, and the posterior basolateral amygdala were taken from three representative sections per mouse at Bregma −2.18 [44]. Images were taken as grayscale 8-bit tiffs with an Optronics MicroFire (Optronics, Goleta, California) digital camera mounted on a Zeiss Axiophot microscope using a Zeiss 10x Plan neofluor NA 0.3 objective and picture frame software. All images were taken with a 2-second exposure and a flat field correction was applied. Analysis was performed with ImageJ 1.46. The scale was set to 1.365 pixels per micron. Measurements are set to measure area and area fraction. The posterior parietal association cortex and the CA1 area of the HPC were framed so that the arch of the anatomy crossed the field diagonally. The basolateral amygdala was centered in the field. Selections outlining the anatomy were made with the polygon tool for cortex and HPC. Due to shape changes, the amygdala was sampled with three unique samples with a circular area of 41145 μm. After the region was selected, the threshold tool was set to 0–150s and applied to create a 2-bit image. Measurements of each region were collected and saved. Mean percent area of 6E10-positive immunoreactivity for each of the three brain regions for male and female 3xTg-AD mice were compared statistically.

Statistical Analyses

Data were analyzed using linear mixed models (proc mixed) using SAS statistical software. *In situ* hybridization data were analyzed with two-way ANOVAs (genotype x sex) for all brain regions, except the HPC in which 3-way ANOVAs were used (genotype x sex x HPC subregion). CORT radioimmunoassay and behavioral data were analyzed with two-way ANOVAs (genotype x sex). Post hoc least-squared means tests with slices were performed to determine effects of genotype and sex in specific groups. 6E10 immunohistochemistry data were analyzed using t-tests to compare sex differences. The significance value for all tests was $\alpha < 0.05$.

RESULTS

Emotional and Anxiety-Like Behavior

In the EPM, a commonly used test of anxiety-like behavior, both WT and 3xTg-AD six-month-old mice showed similar levels of avoidance of the open arms as nearly half the males and more than half the females either never entered the open arms at all or they froze when they did enter an open arm (Figure 1A). Interestingly, only WT mice froze in the open arms (see checkered boxes in Figure 1A). Further, no genotype or sex differences were found in the distance traveled (genotype: $F_{(1/26)}=0$, p=0.97; sex: $F_{(1/26)}=0.51$, p=0.48; Figure 1B) or the total number of entries into all the arms (genotype: $F_{(1/26)}=0.00$, p=0.98; sex: $F_{(1/26)}=1.34$, p=0.26; Figure 1C) of the test apparatus over the five-minute test. Thus, both 3xTg-AD and WT mice exhibit similar levels of locomotor activity and avoidance of the "anxiogenic" open arms in the EPM at six months of age.

In the open field, 3xTg-AD and WT mice demonstrated similar levels of locomotor activity throughout the five-minute test (genotype: $F_{(4/130)}= 1.41$, p=0.24; sex: $F_{(4/130)}=1.90$, p=0.17; interval: $F_{(4/130)}=0.24$, p=0.91; Figure 1D). Male 3xTg-AD mice took significantly longer to enter the periphery after initially being placed in the center than all WT mice (genotype: $F_{(1/26)}=4.95$, p<0.05; posthoc tests--male 3xTg-AD vs. male WT: $F_{(1/26)}= 5.88$, p<0.05 and vs. female WT: $t_{(26)}=-2.47$, p<0.05; Figure 1E). Further, male and female 3xTg-AD mice spent more time in the center of the open field than WT mice, especially during the early portion of the test, as shown by significant main effects for genotype ($F_{(1/26)}=7.09$, p=0.01)

and time interval ($F_{(4/104)}$=13.68, p<0.001) and a significant genotype by interval interaction ($F_{(4/104)}$=3.58, p<0.01; Figure 1F). Posthoc tests reveal that male 3xTg-AD mice spent more time in the center than male WT mice during the first minute ($F_{(1/104)}$=6.20, p=0.01), while female 3xTg-AD mice spent more time in the center than female WT mice during the second and third minutes (second: $F_{(1/104)}$=6.92, p<0.01 and third: $F_{(1/104)}$=4.75, p=0.05) and more time than male 3xTg-AD mice during the second minute of the test ($F_{(1/104)}$=5.70, p<0.05). This increased time spent in the center by the 3xTg-AD mice was accompanied by a slower speed of movement (i.e., decreased velocity) early in the test, as revealed by significant main effects for genotype ($F_{(1/26)}$=4.55, p<0.05) and interval ($F_{(4/81)}$=18.72, p<0.001). Posthoc analyses reveal that female 3xTg-AD mice moved slower than female WT mice in the center during the first and second minutes (first: $F_{(1/81)}$=3.58, p=0.06; second: $F_{(1/81)}$=4.54, p<0.05), while the male 3xTg-AD mice moved significantly slower than female WT mice during the first minute ($t_{(81)}$=2.13, p<0.05; Figure 1G). However, the 3xTg-AD mice did not freeze in the center as their latency to move when first placed in the open field did not differ from WT mice ($F_{(1/26)}$=0.76, p=0.39; Table 1) and their mean velocity was greater than 7 cm per second. These data show that male and female 3xTg-AD mice exhibit a mild disinhibition of behavior in the open field at six months of age by spending more time in the center early during the test.

Latency to move after initially being placed in an apparatus and the number of defecation boli were also measured in the EPM and the open field. As mentioned above, 3xTg-AD mice did not differ from WT mice in the latency to move in the open field; however, these transgenic mice did take significantly longer than WT mice to move in the EPM ($F_{(1/26)}$=9.34, p<0.01; Table 1). Mixed model analyses of the number of defecation boli generated during the EPM and open field tests reveal significant effects for genotype but not sex in both tests (EPM--genotype: $F_{(1/26)}$=4.17, p=0.05 and sex: $F_{(1/26)}$=0.01, p=0.94; open field--genotype: $F_{(1/26)}$=7.95, p<0.01 and sex: $F_{(1/26)}$=0.41, p=0.53). Posthoc analyses show that the number of defecation boli generated was significantly higher for male 3xTg-AD mice compared to male WT mice in both the EPM ($F_{(1/26)}$=5.55, p<0.05) and the open field ($F_{(1/26)}$=6.96, p=0.01), but females generated similar numbers of defecation boli (EPM: $F_{(1/26)}$=0.22, p=0.64; open field: $F_{(1/26)}$=1.71, p=0.21; Table 1). Thus, 3xTg-AD mice show altered emotionality at six months of age.

Gene Expression of Stress-Related Molecules

Since dysregulation of the HPA axis may precede substantial Aβ accumulation and consistent behavioral alterations, and serve as a risk factor for AD, regulation of the HPA axis during early stage AD-like pathology in 3–4 month old 3xTg-AD mice was examined via *in situ* hybridization histochemistry of basal gene expression of the stress-related molecules GR, MR, and CRH in brain.

The HPC is a key brain structure involved in learning and memory and turn-off of the stress axis, and shows substantial AD pathology over time. Analysis of MR gene expression reveals that male mice exhibit significantly higher MR mRNA levels in the HPC compared to female mice (subregion dependent upon genotype), as shown by significant effects for sex ($F_{(1/3831)}$=19.04; p<0.001) and subregion ($F_{(3/3831)}$=2612.83, p<0.001), but not genotype ($F_{(1/3831)}$=0.52, p=0.47). In this mixed model analysis, several interactions are also significant (sex by region: $F_{(3/3831)}$=33.00, p<0.001; genotype by region: $F_{(3/3831)}$=9.87, p<0.001; and sex by genotype by region: $F_{(3/3831)}$=7.53, p<0.001). Thus, each hippocampal subregion was also examined separately, revealing significant effects for genotype ($F_{(1/938)}$=7.51, p<0.01) and sex ($F_{(1/938)}$=10.73, p=0.001) in the CA3, the subregion that is highly sensitive to chronic stress [45, 46]. Posthoc tests show that male 3xTg-AD mice exhibit significantly higher MR mRNA expression in the CA3 area compared to their male

WT counterparts ($F_{(1/938)}$=9.08, p<0.01) and all female mice (vs. female 3xTg-AD: $F_{(1/938)}$=10.11, p<0.01 and vs. female WT: t_{938}=−4.33, p<0.001; Figure 2A–C).

Male 3xTg-AD mice also exhibit significantly higher GR mRNA levels in the CA3 and dentate gyrus subregions of the HPC (Figure 2D–G). A mixed model analysis of GR mRNA expression in all hippocampal subregions reveals significant effects for subregion ($F_{(3/3921)}$=2386.21, p<0.001) and several interactions (sex by region: $F_{(3/3921)}$=11.03, p<0.001; genotype by region: $F_{(3/3921)}$=15.72, p<0.001; and sex by genotype by region: $F_{(3/3921)}$=17.73, p<0.001), but not for sex ($F_{(1/3921)}$=2.26, p=0.13) or genotype ($F_{(1/3921)}$=3.03, p=0.08). Given the significant interactions, each hippocampal subregion was also examined separately. A mixed model analysis of the CA3 subregion shows a significant effect for genotype ($F_{(1/956)}$=4.80, p<0.05), but not sex ($F_{(1/956)}$=1.47, p=0.22). Posthoc analysis shows that male 3xTg-AD mice exhibit higher GR mRNA levels in the CA3 subregion compared to their WT counterparts ($F_{(1/956)}$=5.44, p<0.05; Figure 2D, E, and F). A mixed model analysis of the dentate gyrus reveals significant effects for sex ($F_{(1/959)}$=5.58, p<0.05) and genotype ($F_{(1/959)}$=6.87, p<0.01). Posthoc analysis shows that male 3xTg-AD mice exhibit significantly higher GR mRNA levels in the dentate gyrus than all WT mice (vs. females: t_{959}=−3.66, p<0.001; vs. males: $F_{(1/959)}$=4.07, p<0.05; Figure 2D, E, and G). Thus, two areas of the HPC (i.e., CA3 and dentate gyrus) show stress molecule-related changes in gene expression when AD pathology is in the early stages.

GR mRNA expression, along with CRH, were also examined in other stress- and emotionality-related brain regions including the PVN, the CeA and the BST. The PVN is a key structure involved in the modulation of the HPA axis. A mixed model analysis of GR mRNA expression in the PVN shows a significant effect for genotype ($F_{(1/211)}$: 5.59, p<0.05) but not sex ($F_{(1/211)}$: 0.00, p=0.97), and a significant sex by genotype interaction ($F_{(1/211)}$: 4.06, p<0.05). Post hoc tests reveal that male 3xTg-AD mice have significantly higher GR mRNA levels than male WT mice ($F_{(1/211)}$=10.18, p<0.01; Figure 3A, B, and E). In contrast, the opposite is true for CRH mRNA in which male WT mice have significantly more CRH mRNA in the PVN than male 3xTg-AD mice (Figure 3C, D, and F), as revealed by significant effects for genotype ($F_{(1/309)}$=6.02, p=0.01) but not sex ($F_{(1/309)}$=0.01, p=0.93; posthoc tests: M-WT vs. M-3xTg-AD: $F_{(1/309)}$=8.74, p<0.01). Interestingly, female transgenic mice do not show GR or CRH changes in the PVN.

The primary role of the CeA is the modulation of fear and anxiety-like responses. A mixed model analysis of GR mRNA expression in the CeA reveals significant main effects for sex ($F_{(1/1152)}$: 9.98, p<0.01) and genotype ($F_{(1/1152)}$: 7.18, p<0.01) and a significant sex by genotype interaction ($F_{(1/1152)}$: 26.88, p<0.001). Posthoc analysis shows that female 3xTg-AD mice exhibit higher GR mRNA levels in the CeA than their male transgenic counterparts ($F_{(1/1152)}$=31.79, p<0.001) and all WT mice (vs. F-WT: $F_{(1/1152)}$=27.08, p<0.001; vs. M-WT: t_{1152}=3.96, p<0.001; Figure 4A, B, and E). Interestingly, the male 3xTg-AD mice do not show increased GR mRNA expression in this brain region. However, both male and female 3xTg-AD mice do show significantly more CRH mRNA expression than WT mice in the CeA (Figure 4C, D, and F). A mixed model analysis of CRH mRNA in the CeA reveals a significant effect for genotype ($F_{(1/408)}$=26.23, p<0.001), but not sex ($F_{(1/408)}$=0.06, p=0.81). This increased mRNA expression is strongest in the rostral part of this nucleus, similar to what we have reported in our GR overexpressing (GRov) mice that show increased anxiety-like behavior [47]. Posthoc analysis shows that female and male 3xTg-AD mice have significantly more CRH mRNA expression in the rostral part of the CeA compared to female ($F_{(1/408)}$=17.10, p<0.001) and male ($F_{(1/408)}$=9.32, p<0.01) WT mice.

The BST is the major relay between the HPC (the main extra-hypothalamic negative feedback regulator of the HPA axis) and the PVN. The BST is also considered part of the extended amygdala since it plays a role in emotional behavior. Analysis of the *in situ* hybridization data reveals both sex and genotype differences in CRH mRNA expression in the dorsolateral BST (BSTLD). A mixed model analysis of the dorsal BST (dorsomedial and dorsolateral regions) reveals significant effects for sex ($F_{(1/459)}$=6.03, p=0.01), genotype ($F_{(1/459)}$=11.44, p<0.001), region ($F_{(1/459)}$=45.95, p<0.001), and a genotype by region interaction ($F_{(1/459)}$=6.11, p=0.01). Posthoc analysis shows that female and male 3xTg-AD mice exhibit significantly more CRH mRNA expression in the BSTLD when compared to WT mice (Females: $F_{(1/459)}$=5.20, p<0.05; Males: $F_{(1/459)}$=12.38, p<0.001; Figure 5A–D). In addition, male 3xTgAD mice express even more CRH mRNA in the BSTLD than their female transgenic counterparts ($F_{(1/459)}$=5.30, p<0.05).

Glucocorticoid Levels

In contrast to gene expression of stress-related molecules in brain, basal plasma CORT levels in the 3–4 month old 3xTg-AD mice are not different from their WT counterparts, but females exhibit higher levels than males (Table 2). A mixed model analysis reveals a significant effect for sex ($F_{(1/30)}$=14.72, p<0.001), but not genotype ($F_{(1/30)}$=0.4144, p=0.41). In the six-month-old mice that underwent behavioral testing, basal CORT levels were also similar between 3xTg-AD and male WT mice. A mixed model analysis of the six-month-old mice also reveals a significant effect for sex ($F_{(1/22)}$= 6.61, p<0.05), but not genotype ($F_{(1/22)}$= 0.91, p<0.35). A sex by genotype interaction is also significant ($F_{(1/22)}$= 4.57, p<0.05). Posthoc analyses reveal that female WT mice exhibited higher CORT levels than all other mice (female WT vs. male WT: $F_{(1/22)}$=11.09, p<0.01; vs. female 3xTg-AD: $F_{(1/22)}$=5.19, p<0.05; vs. male 3xTg-AD: $t_{(22)}$=2.49, p<0.05). CORT values show high variability among six-month-old female WT mice. Nevertheless, male and female 3xTg-AD mice do not show elevated basal CORT levels at these young ages.

Neuroanatomical Expression of hβAPP/Aβ Pathology

Adjacent sections to those used for examining gene expression of stress-related molecules in the 3–4-month-old 3xTg-AD mice were stained with the 6E10 antibody to assess hAβPP/Aβ neuropathology. No hAβPP/Aβ pathology was found in the PVN, BST, or CeA. Representative images from the HPC and posterior parietal association cortex (A and B), and posterior basolateral amygdala (C and D) at Bregma −2.18 [44] are shown in Figure 6A–D. 6E10 immunoreactivity is found in the pyramidal cell layer of the CA1–CA3 areas of the hippocampus and layers IV and V of the cortex. At this age, hAβPP/Aβ staining is limited to the cell bodies, with little to no staining of fibers in the stratum radiatum or oriens of the HPC. Importantly, no 6E10 immunopositive plaques were found, indicating an early stage of pathology in these animals. When examining the percent area of 6E10 immunopositive cells, female 3xTg-AD mice exhibited significantly higher 6E10 immunoreactivity in the CA1 area of the HPC ($t_{(53)}$=8.81, p<0.001) and basolateral amygdala ($t_{(107)}$=3.77, p<0.001) compared to male 3xTg-AD mice (Figure 6E). In contrast, 6E10 immunoreactivity was similar between males and females in the posterior parietal association cortex ($t_{(53)}$= −0.81, p=0.42). Thus, even during early-stage pathology at 3–4 months of age in the 3xTg-AD mouse model, females show more hβAPP/Aβ pathology in the HPC and amygdala than males.

DISCUSSION

The results of the present study clearly demonstrate that: 1) the central stress axis of young 3xTg-AD mice shows activation at the gene expression level in several brain areas at a time of early-stage neuropathology and mild behavioral alterations, and 2) these stress-gene

expression changes exist concurrently with normal circulating CORT levels. Young male 3xTg-AD mice exhibit significantly higher basal MR and GR mRNA levels in the HPC and increased GR but decreased CRH mRNA levels in the PVN compared to male WT mice. Both male and female 3xTg-AD mice exhibit significantly higher CRH mRNA levels in the CeA and BSTLD than WT mice, with females also showing higher GR mRNA levels in the CeA. The finding that the central HPA axis is activated basally in young early-stage AD pathologic mice suggests that HPA axis changes may begin before the appearance of overt brain pathology. Further studies to determine the timing of the onset of such central HPA axis changes in comparison to AD-like pathology are warranted since early HPA axis alterations may possibly serve as an antecedent factor for individuals at high risk for AD before Aβ accumulation is detected. The identification of such early-stage antecedent factors is critical for the development of AD prevention strategies because the onset of neuropathological abnormalities precedes the appearance of cognitive and neuropsychiatric symptoms by many years [3, 4].

The central stress molecule gene expression changes reported here are present in naïve 3xTg-AD mice that have not experienced any type of environmental or experimental manipulation. Since a central function of our bodies is to maintain homeostasis at all levels, including the HPA axis, these young animals with early-stage pathology and mild behavioral alterations are likely exhibiting physiological regulation to achieve homeostasis. These regulatory changes in the HPA axis are found at the central level, which over time or exposure to threatening conditions may become increasingly difficult for the animal to maintain. As a result, the animal may experience increasing susceptibility for neuronal dysfunction with resultant changes in emotional and cognitive behavior. Some evidence for regulatory changes in other systems of young 3xTg-AD mice has been reported. Brain oxidative stress is increased in 3–5-month-old female 3xTg-AD mice [48]. Changes in inflammatory factors in the peripheral immune system and brain are found in 5–6-month-old 3xTg-AD mice [49]. 3xTg-AD mice also exhibit alterations in calcium signaling as early as six weeks of age, yet synaptic function does not appear to be disrupted [50, 51]. Thus, the key finding of an activated central stress axis in these young 3xTg-AD mice may reflect a phenotype with a heightened allostatic load [52], in which an organism experiences wear and tear on the brain and body resulting from chronic overactivity or underactivity of physiological systems that normally serve adaptive functions to internal and external challenges. The control of the HPA or stress axis is especially important, because when this system does not turn off over time, it can cause damage or promote pathology.

The stress molecule gene expression alterations in the brains of young 3xTg-AD mice point to an activated HPA axis like that found with chronic stress. During chronic stress, CRH is upregulated in the CeA and BST [53, 54], as observed basally in the 3–4-month-old 3xTg-AD mice. However, CRH levels in the PVN are increased, decreased, or not changed depending upon the type of stress [53–56] along with a corresponding change in GR mRNA levels in the opposite direction [57]. In the current study, young male 3xTg-AD mice showed decreased basal CRH levels with a concomitant increase in GR mRNA in the PVN and HPC, consistent with negative feedback onto the HPA axis in the basal state. Reduction of CRH synthesis and activity in the PVN after stress is thought to be essential in limiting the stress response and preventing pathologies associated with excess CRH levels [57, 58]. Male 3xTg-AD mice show such reduction in CRH synthesis in the PVN, suggesting that they possess a tight feedback of the HPA axis at this young age. Nevertheless, such physiological regulation of the HPA axis as demonstrated by increased CRH in the CeA and BST and the changes in the PVN resulting from prolonged exposure to stressors, or as observed in the basal state of young early-pathologic male 3xTg-AD mice, may lead over time to development of a maladaptive “chronic stress state” and contribute to changes at the neuronal and behavioral levels. Chronic hyperactivation of the CRH system, for example, is

associated with stress-related psychiatric disorders such as anxiety and depression [59, 60]. Further, an optimal level of glucocorticoid signaling is required for normal brain function and deviation from this optimal level in either direction, as observed in young male 3xTg-AD mice with increased MR and GR gene expression in the HPC, is extremely harmful over time to neuronal integrity [9].

These gene expression changes in the central HPA axis in young 3xTg-AD mice occur simultaneously with normal circulating plasma CORT levels. Alterations in peripheral circulating CORT levels do not necessarily accompany central HPA axis alterations. For example, aged animals show HPA axis regulation through the interplay of multiple levels of control resulting in normal circulating levels of CORT under resting conditions [24, 61]. Young forebrain glucocorticoid-overexpressing mice (GRov mice) also show such an aging-like neuroendocrine phenotype with normal levels of circulating stress hormones under resting conditions [62]. However, under stress conditions, these same aged and transgenic animals show a delayed recovery to basal CORT levels even hours after the termination of the stressor [24, 62, 63]. Thus, given the central HPA axis changes in the young 3xTg-AD mice found here, especially in the HPC and BST, one would hypothesize that these young mice would eventually show impaired negative feedback with a delay in the turn-off of the HPA axis following stress. This appears to be the case because at 12 months of age, the 3xTg-AD mice show attenuated habituation to chronic mild social stress as evidenced by elevated CORT levels compared to WT mice, with resulting exacerbation of Aβ pathology [64]. Although exogenous dexamethasone exacerbates Aβ pathology in four-month-old 3xTg-AD mice [33], further studies are needed to determine the impact of acute and chronic naturalistic stressors at younger ages in this mouse model. In the basal state, our data show that 3xTg-AD mice show normal circulating CORT levels at least until nine months of age (data not shown), but an activated central stress axis as early as three months of age.

Non-cognitive symptoms of AD, termed the Behavioral and Psychological Symptoms of Dementia (BPSD), are frequently observed and affect more than 80% of patients over the course of the illness [65]. Activity disturbance is the most prevalent symptom observed in nearly all early AD subjects, with anxiety the next most frequent symptom [64]. Apathy, aberrant motor activity, dysphoria and anxiety are the symptoms most frequently reported by caregivers [67]. The majority of the BPSD symptoms that are present with a mild degree of dementia consistently persist, or even increase in severity, into the later stages of dementia [66, 67]. Importantly, increased emotionality and other BPSD precede cognitive impairment by several years [41], and may be considered as predictive symptoms leading to dementia. The early manifestations of BPSD in AD and their persistence over the disease trajectory stand in contrast to the rather linear decline in cognitive functions over time. This dissociation between the manifestations of cognitive and non-cognitive symptoms suggests that independent pathological mechanisms are involved [68]. Factors likely to cause manifestations of BPSD are environmental changes, genetic predisposition, past history of adversity and stress exposure, or individual differences in response to stress.

Gene expression changes in the central stress axis, like that found in the young 3xTg-AD mice of the current study, may play a role in the manifestations of BPSD. Thus, we chose to examine molecular and behavioral correlates of emotionality in 3xTg-AD mice. Consistent among both male and female 3xTg-AD mice is the upregulation of CRH mRNA expression in the emotionality-related brain regions CeA and BST. Female 3xTg-AD mice also express higher GR mRNA levels in the CeA. The amygdala and BST are highly interconnected, and distinct subregions are considered to be part of the “extended amygdala” [15]. The BST plays a special role in longer-duration, sustained, anxiety-like responses while the CeA mediates shorter duration fear (threat) responses [16]. Elevated CRH mRNA levels are found in the CeA and lateral BST (especially the dorsolateral division) upon exposure to

innate fear and anxiety tests [16, 69]. Both the CeA and the BST receive projections from the basolateral amygdala [70], which screens incoming sensory information for threat cues and shows AβPP/Aβ accumulation in AD transgenic mouse models such as the 3xTg-AD mice used in the current study.

Increased emotionality and anxiety-like behaviors have been reported in 3xTg-AD mice with an increase in severity with advancing age [37, 43, 71]. Six-month-old 3xTg-AD mice in the current study did not show anxiety-like behavior in the EPM, but exhibited altered emotionality on two indices: increased defecation and reduced initial exploratory behavior in the EPM, which is consistent with some reports [43, 72]. However, contrary to others [37, 43], these mice showed a mild disinhibition in the open field by spending more time in the center and did not exhibit freezing behavior. These mice also exhibited similar levels of locomotor activity to that of the WT mice, which is also contrary to the reported decreased ambulation [37, 40, 43, 71]. The current data suggest mild behavioral changes in 3xTg-AD mice at six months of age, which would likely be even milder at the age (3–4 months) at which gene expression of stress-related molecules was examined. We have detected alterations in gene expression (i.e., GR and CRH) in stress- and emotionality-related brain areas that predate the emergence of substantial behavioral changes. Such gene alterations may indicate a vulnerability to altered emotionality or anxiety-like behavior similar to that observed in humans with AD.

The male 3xTg-AD phenotype of an activated central stress axis at the gene expression level (i.e., GR, MR, CRH) involves the HPC, PVN, CeA, and BST, while the female 3xTg-AD phenotype is limited to the CeA and BST. The increased CRH mRNA levels in the CeA and BST found in both sexes is likely tied to the eventual heightened emotionality and anxiety phenotype of these mice, and the additional increased GR levels in the CeA for the females may play a role in the more severe BPSD behaviors observed in females as compared to males [37]. In contrast, females do not show alterations of the HPA axis at the level of the PVN and the HPC, suggesting that 3xTg-AD males exhibit a tighter feedback of the HPA axis at 3–4 months of age. These young female 3xTg-AD mice also exhibit more hAβPP/Aβ in the HPC and amygdala than males, which is consistent with other reports of more extensive neuropathology and cognitive impairments in female 3xTg-AD mice [37–40, 73]. One can speculate that the tighter feedback on the HPA axis to maintain homeostasis in male 3xTg-AD mice early in life may at least temporarily curtail pathological acceleration relative to females.

In summary, our findings reveal an activated central HPA axis, as measured by alterations of stress-related molecules, in young 3xTg-AD mice with early-stage AD neuropathology and mild behavioral alterations. These data impart a phenotype to the 3xTg-AD mouse model suggestive of a heightened allostatic load or vulnerability to stress at a very early age. These early alterations are prime targets for determining useful antecedent factors for those at high risk of developing AD or, in the case of the HPA axis alterations, those at high risk for developing certain AD-associated behavioral deficits related to altered emotionality.

Acknowledgments

This work was supported by an Alzheimer's Association Grant IIRG-07-59991 (E.K.H-B.) and NIDA 5 P01 DA021633 (H.A.). The authors would like to thank Linda Dokas and Audrey Seasholtz for critical reading of the manuscript.

References

1. Herman JP, Seroogy K. Hypothalamic-pituitary-adrenal axis, glucocorticoids, and neurologic disease. Neurol Clin. 2006; 24:461–481. vi. [PubMed: 16877118]

2. Hebert LE, Scherr PA, Bienias JL, Bennett DA, Evans DA. Alzheimer disease in the US population: prevalence estimates using the 2000 census. Arch Neurol. 2003; 60:1119–1122. [PubMed: 12925369]
3. Braak H, Braak E. Neuropathological stageing of Alzheimer-related changes. Acta Neuropathol. 1991; 82:239–259. [PubMed: 1759558]
4. Thal DR, Rub U, Orantes M, Braak H. Phases of A beta-deposition in the human brain and its relevance for the development of AD. Neurology. 2002; 58:1791–1800. [PubMed: 12084879]
5. McEwen BS. Protection and damage from acute and chronic stress: allostasis and allostatic overload and relevance to the pathophysiology of psychiatric disorders. Ann N Y Acad Sci. 2004; 1032:1–7. [PubMed: 15677391]
6. Lupien SJ, Nair NP, Briere S, Maheu F, Tu MT, Lemay M, McEwen BS, Meaney MJ. Increased cortisol levels and impaired cognition in human aging: implication for depression and dementia in later life. Rev Neurosci. 1999; 10:117–139. [PubMed: 10658955]
7. Akil, H.; Morano, MI. The Biology of Stress: From Periphery to Brain. In: Watson, SJ., editor. Biology of Schizophrenia and Affective Disease. Raven Press; New York: 1996. p. 15-48.
8. Akil H. Stressed and depressed. Nat Med. 2005; 11:116–118. [PubMed: 15692589]
9. De Kloet ER, Vreugdenhil E, Oitzl MS, Joels M. Brain corticosteroid receptor balance in health and disease. Endocrine Reviews. 1998; 19:269–301. [PubMed: 9626555]
10. Caamano CA, Morano MI, Akil H. Corticosteroid receptors: a dynamic interplay between protein folding and homeostatic control. Possible implications in psychiatric disorders. Psychopharmacology Bulletin. 2001; 35:6–23. [PubMed: 12397867]
11. Herman JP, Ostrander MM, Mueller NK, Figueiredo H. Limbic system mechanisms of stress regulation: hypothalamo-pituitary-adrenocortical axis. Prog Neuropsychopharmacol Biol Psychiatry. 2005; 29:1201–1213. [PubMed: 16271821]
12. Cullinan WE, Herman JP, Watson SJ. Ventral subicular interaction with the hypothalamic paraventricular nucleus: evidence for a relay in the bed nucleus of the stria terminalis. J Comp Neurol. 1993; 332:1–20. [PubMed: 7685778]
13. Prewitt CM, Herman JP. Anatomical interactions between the central amygdaloid nucleus and the hypothalamic paraventricular nucleus of the rat: a dual tract-tracing analysis. J Chem Neuroanat. 1998; 15:173–185. [PubMed: 9797074]
14. Spencer SJ, Buller KM, Day TA. Medial prefrontal cortex control of the paraventricular hypothalamic nucleus response to psychological stress: possible role of the bed nucleus of the stria terminalis. J Comp Neurol. 2005; 481:363–376. [PubMed: 15593338]
15. Alheid GF. Extended amygdala and basal forebrain. Ann N Y Acad Sci. 2003; 985:185–205. [PubMed: 12724159]
16. Walker DL, Miles LA, Davis M. Selective participation of the bed nucleus of the stria terminalis and CRF in sustained anxiety-like versus phasic fear-like responses. Prog Neuropsychopharmacol Biol Psychiatry. 2009; 33:1291–1308. [PubMed: 19595731]
17. Wilson RS, Begeny CT, Boyle PA, Schneider JA, Bennett DA. Vulnerability to stress, anxiety, and development of dementia in old age. Am J Geriatr Psychiatry. 2011; 19:327–334. [PubMed: 21427641]
18. Wilson RS, Arnold SE, Schneider JA, Li Y, Bennett DA. Chronic distress, age-related neuropathology, and late-life dementia. Psychosom Med. 2007; 69:47–53. [PubMed: 17244848]
19. Johansson L, Guo X, Waern M, Ostling S, Gustafson D, Bengtsson C, Skoog I. Midlife psychological stress and risk of dementia: a 35-year longitudinal population study. Brain. 2010; 133:2217–2224. [PubMed: 20488887]
20. Magri F, Cravello L, Barili L, Sarra S, Cinchetti W, Salmoiraghi F, Micale G, Ferrari E. Stress and dementia: the role of the hypothalamicpituitary-adrenal axis. Aging Clin Exp Res. 2006; 18:167–170. [PubMed: 16702789]
21. Nasman B, Olsson T, Viitanen M, Carlstrom K. A subtle disturbance in the feedback regulation of the hypothalamic-pituitary-adrenal axis in the early phase of Alzheimer's disease. Psychoneuroendocrinology. 1995; 20:211–220. [PubMed: 7899539]

22. Born J, Ditschuneit I, Schreiber M, Dodt C, Fehm HL. Effects of age and gender on pituitary-adrenocortical responsiveness in humans. Eur J Endocrinol. 1995; 132:705–711. [PubMed: 7788010]

23. Kudielka BM, Schmidt-Reinwald AK, Hellhammer DH, Kirschbaum C. Psychological and endocrine responses to psychosocial stress and dexamethasone/corticotropin-releasing hormone in healthy postmenopausal women and young controls: the impact of age and a two-week estradiol treatment. Neuroendocrinology. 1999; 70:422–430. [PubMed: 10657735]

24. Morano MI, Vazquez DM, Akil H. The role of the hippocampal mineralocorticoid and glucocorticoid receptors in the hypothalamo-pituitary-adrenal axis of the aged Fisher rat. Mol Cell Neurosci. 1994; 5:400–412. [PubMed: 7820364]

25. Carroll JC, Iba M, Bangasser DA, Valentino RJ, James MJ, Brunden KR, Lee VM, Trojanowski JQ. Chronic stress exacerbates tau pathology, neurodegeneration, and cognitive performance through a corticotropin-releasing factor receptor-dependent mechanism in a transgenic mouse model of tauopathy. J Neurosci. 2011; 31:14436–14449. [PubMed: 21976528]

26. Catania C, Sotiropoulos I, Silva R, Onofri C, Breen KC, Sousa N, Almeida OF. The amyloidogenic potential and behavioral correlates of stress. Mol Psychiatry. 2009; 14:95–105. [PubMed: 17912249]

27. Cuadrado-Tejedor M, Ricobaraza A, Frechilla D, Franco R, Perez-Mediavilla A, Garcia-Osta A. Chronic Mild Stress Accelerates the Onset and Progression of the Alzheimer's Disease Phenotype in Tg2576 Mice. J Alzheimers Dis. 2011

28. Dong H, Goico B, Martin M, Csernansky CA, Bertchume A, Csernansky JG. Modulation of hippocampal cell proliferation, memory, and amyloid plaque deposition in APPsw (Tg2576) mutant mice by isolation stress. Neuroscience. 2004; 127:601–609. [PubMed: 15283960]

29. Jeong YH, Park CH, Yoo J, Shin KY, Ahn SM, Kim HS, Lee SH, Emson PC, Suh YH. Chronic stress accelerates learning and memory impairments and increases amyloid deposition in APPV717I-CT100 transgenic mice, an Alzheimer's disease model. FASEB J. 2006; 20:729–731. [PubMed: 16467370]

30. Srivareerat M, Tran TT, Alzoubi KH, Alkadhi KA. Chronic psychosocial stress exacerbates impairment of cognition and long-term potentiation in beta-amyloid rat model of Alzheimer's disease. Biol Psychiatry. 2009; 65:918–926. [PubMed: 18849021]

31. Tran TT, Srivareerat M, Alkadhi KA. Chronic psychosocial stress accelerates impairment of long-term memory and late-phase long-term potentiation in an at-risk model of Alzheimer's disease. Hippocampus. 2011; 21:724–732. [PubMed: 20865724]

32. Dong H, Yuede CM, Yoo HS, Martin MV, Deal C, Mace AG, Csernansky JG. Corticosterone and related receptor expression are associated with increased beta-amyloid plaques in isolated Tg2576 mice. Neuroscience. 2008; 155:154–163. [PubMed: 18571864]

33. Green KN, Billings LM, Roozendaal B, McGaugh JL, LaFerla FM. Glucocorticoids increase amyloid-beta and tau pathology in a mouse model of Alzheimer's disease. J Neurosci. 2006; 26:9047–9056. [PubMed: 16943563]

34. Lee KW, Kim JB, Seo JS, Kim TK, Im JY, Baek IS, Kim KS, Lee JK, Han PL. Behavioral stress accelerates plaque pathogenesis in the brain of Tg2576 mice via generation of metabolic oxidative stress. J Neurochem. 2009; 108:165–175. [PubMed: 19012747]

35. Sotiropoulos I, Catania C, Pinto LG, Silva R, Pollerberg GE, Takashima A, Sousa N, Almeida OF. Stress acts cumulatively to precipitate Alzheimer's disease-like tau pathology and cognitive deficits. J Neurosci. 2011; 31:7840–7847. [PubMed: 21613497]

36. Oddo S, Caccamo A, Shepherd JD, Murphy MP, Golde TE, Kayed R, Metherate R, Mattson MP, Akbari Y, LaFerla FM. Triple-transgenic model of Alzheimer's disease with plaques and tangles: intracellular Abeta and synaptic dysfunction. Neuron. 2003; 39:409–421. [PubMed: 12895417]

37. Garcia-Mesa Y, Lopez-Ramos JC, Gimenez-Llort L, Revilla S, Guerra R, Gruart A, Laferla FM, Cristofol R, Delgado-Garcia JM, Sanfeliu C. Physical exercise protects against Alzheimer's disease in 3xTg-AD mice. J Alzheimers Dis. 2011; 24:421–454. [PubMed: 21297257]

38. Gimenez-Llort L, Garcia Y, Buccieri K, Revilla S, Sunol C, Cristofol R, Sanfeliu C. Gender-Specific Neuroimmunoendocrine Response to Treadmill Exercise in 3xTg-AD Mice. Int J Alzheimers Dis. 2010; 2010:128354. [PubMed: 20981262]

39. Hirata-Fukae C, Li HF, Hoe HS, Gray AJ, Minami SS, Hamada K, Niikura T, Hua F, Tsukagoshi-Nagai H, Horikoshi-Sakuraba Y, Mughal M, Rebeck GW, LaFerla FM, Mattson MP, Iwata N, Saido TC, Klein WL, Duff KE, Aisen PS, Matsuoka Y. Females exhibit more extensive amyloid, but not tau, pathology in an Alzheimer transgenic model. Brain Res. 2008; 1216:92–103. [PubMed: 18486110]
40. Pietropaolo S, Sun Y, Li R, Brana C, Feldon J, Yee BK. Limited impact of social isolation on Alzheimer-like symptoms in a triple transgenic mouse model. Behav Neurosci. 2009; 123:181–195. [PubMed: 19170443]
41. Jost BC, Grossberg GT. The evolution of psychiatric symptoms in Alzheimer's disease: a natural history study. J Am Geriatr Soc. 1996; 44:1078–1081. [PubMed: 8790235]
42. Mastrangelo MA, Bowers WJ. Detailed immunohistochemical characterization of temporal and spatial progression of Alzheimer's disease-related pathologies in male triple-transgenic mice. BMC Neurosci. 2008; 9:81. [PubMed: 18700006]
43. Gimenez-Llort L, Blazquez G, Canete T, Johansson B, Oddo S, Tobena A, LaFerla FM, Fernandez-Teruel A. Modeling behavioral and neuronal symptoms of Alzheimer's disease in mice: a role for intraneuronal amyloid. Neurosci Biobehav Rev. 2007; 31:125–147. [PubMed: 17055579]
44. Paxinos, G.; Franklin, KBJ. The Mouse Brain in Stereotaxic Coordinates. Academic Press; San Diego: 2001.
45. McLaughlin KJ, Gomez JL, Baran SE, Conrad CD. The effects of chronic stress on hippocampal morphology and function: an evaluation of chronic restraint paradigms. Brain Res. 2007; 1161:56–64. [PubMed: 17603026]
46. Wang XD, Chen Y, Wolf M, Wagner KV, Liebl C, Scharf SH, Harbich D, Mayer B, Wurst W, Holsboer F, Deussing JM, Baram TZ, Muller MB, Schmidt MV. Forebrain CRHR1 deficiency attenuates chronic stress-induced cognitive deficits and dendritic remodeling. Neurobiol Dis. 2011; 42:300–310. [PubMed: 21296667]
47. Wei Q, Lu XY, Liu L, Schafer G, Shieh KR, Burke S, Robinson TE, Watson SJ, Seasholtz AF, Akil H. Glucocorticoid receptor overexpression in forebrain: a mouse model of increased emotional lability. Proc Natl Acad Sci U S A. 2004; 101:11851–11856. [PubMed: 15280545]
48. Resende R, Moreira PI, Proenca T, Deshpande A, Busciglio J, Pereira C, Oliveira CR. Brain oxidative stress in a triple-transgenic mouse model of Alzheimer disease. Free Radic Biol Med. 2008; 44:2051–2057. [PubMed: 18423383]
49. Subramanian S, Ayala P, Wadsworth TL, Harris CJ, Vandenbark AA, Quinn JF, Offner H. CCR6: a biomarker for Alzheimer's-like disease in a triple transgenic mouse model. J Alzheimers Dis. 2010; 22:619–629. [PubMed: 20847401]
50. Chakroborty S, Goussakov I, Miller MB, Stutzmann GE. Deviant ryanodine receptor-mediated calcium release resets synaptic homeostasis in presymptomatic 3xTg-AD mice. J Neurosci. 2009; 29:9458–9470. [PubMed: 19641109]
51. Stutzmann GE, Smith I, Caccamo A, Oddo S, Laferla FM, Parker I. Enhanced ryanodine receptor recruitment contributes to Ca2+ disruptions in young, adult, and aged Alzheimer's disease mice. J Neurosci. 2006; 26:5180–5189. [PubMed: 16687509]
52. McEwen BS. Stress, adaptation, and disease. Allostasis and allostatic load. Ann N Y Acad Sci. 1998; 840:33–44. [PubMed: 9629234]
53. Albeck DS, McKittrick CR, Blanchard DC, Blanchard RJ, Nikulina J, McEwen BS, Sakai RR. Chronic social stress alters levels of corticotropin-releasing factor and arginine vasopressin mRNA in rat brain. J Neurosci. 1997; 17:4895–4903. [PubMed: 9169547]
54. Makino S, Gold PW, Schulkin J. Effects of corticosterone on CRH mRNA and content in the bed nucleus of the stria terminalis; comparison with the effects in the central nucleus of the amygdala and the paraventricular nucleus of the hypothalamus. Brain Res. 1994; 657:141–149. [PubMed: 7820612]
55. Erhardt A, Muller MB, Rodel A, Welt T, Ohl F, Holsboer F, Keck ME. Consequences of chronic social stress on behaviour and vasopressin gene expression in the PVN of DBA/2OlaHsd mice--influence of treatment with the CRHR1-antagonist R121919/NBI 30775. J Psychopharmacol. 2009; 23:31–39. [PubMed: 18515457]

56. Romeo RD, Karatsoreos IN, Jasnow AM, McEwen BS. Age- and stress-induced changes in corticotropin-releasing hormone mRNA expression in the paraventricular nucleus of the hypothalamus. Neuroendocrinology. 2007; 85:199–206. [PubMed: 17505125]
57. Makino S, Hashimoto K, Gold PW. Multiple feedback mechanisms activating corticotropin-releasing hormone system in the brain during stress. Pharmacol Biochem Behav. 2002; 73:147–158. [PubMed: 12076734]
58. Aguilera G, Kiss A, Liu Y, Kamitakahara A. Negative regulation of corticotropin releasing factor expression and limitation of stress response. Stress. 2007; 10:153–161. [PubMed: 17514584]
59. Bale TL. Sensitivity to stress: dysregulation of CRF pathways and disease development. Horm Behav. 2005; 48:1–10. [PubMed: 15919381]
60. Heinrichs SC, Koob GF. Corticotropin-releasing factor in brain: a role in activation, arousal, and affect regulation. J Pharmacol Exp Ther. 2004; 311:427–440. [PubMed: 15297468]
61. Herman JP, Larson BR, Speert DB, Seasholtz AF. Hypothalamo-pituitary-adrenocortical dysregulation in aging F344/Brown-Norway F1 hybrid rats. Neurobiol Aging. 2001; 22:323–332. [PubMed: 11182482]
62. Wei Q, Hebda-Bauer EK, Pletsch A, Luo J, Hoversten MT, Osetek AJ, Evans SJ, Watson SJ, Seasholtz AF, Akil H. Overexpressing the glucocorticoid receptor in forebrain causes an aging-like neuroendocrine phenotype and mild cognitive dysfunction. J Neurosci. 2007; 27:8836–8844. [PubMed: 17699665]
63. Bizon JL, Helm KA, Han JS, Chun HJ, Pucilowska J, Lund PK, Gallagher M. Hypothalamic-pituitary-adrenal axis function and corticosterone receptor expression in behaviourally characterized young and aged Long-Evans rats. Eur J Neurosci. 2001; 14:1739–1751. [PubMed: 11860468]
64. Rothman SM, Herdener N, Camandola S, Texel SJ, Mughal MR, Cong WN, Martin B, Mattson MP. 3xTgAD mice exhibit altered behavior and elevated Abeta after chronic mild social stress. Neurobiol Aging. 2012; 33:830 e831–812. [PubMed: 21855175]
65. Mega MS, Cummings JL, Fiorello T, Gornbein J. The spectrum of behavioral changes in Alzheimer's disease. Neurology. 1996; 46:130–135. [PubMed: 8559361]
66. Eustace A, Coen R, Walsh C, Cunningham CJ, Walsh JB, Coakley D, Lawlor BA. A longitudinal evaluation of behavioural and psychological symptoms of probable Alzheimer's disease. Int J Geriatr Psychiatry. 2002; 17:968–973. [PubMed: 12325059]
67. Piccininni M, Di Carlo A, Baldereschi M, Zaccara G, Inzitari D. Behavioral and psychological symptoms in Alzheimer's disease: frequency and relationship with duration and severity of the disease. Dement Geriatr Cogn Disord. 2005; 19:276–281. [PubMed: 15775717]
68. Casanova MF, Starkstein SE, Jellinger KA. Clinicopathological correlates of behavioral and psychological symptoms of dementia. Acta Neuropathol. 2011; 122:117–135. [PubMed: 21455688]
69. Shepard JD, Barron KW, Myers DA. Corticosterone delivery to the amygdala increases corticotropin-releasing factor mRNA in the central amygdaloid nucleus and anxiety-like behavior. Brain Res. 2000; 861:288–295. [PubMed: 10760490]
70. Dong HW, Petrovich GD, Swanson LW. Topography of projections from amygdala to bed nuclei of the stria terminalis. Brain Res Brain Res Rev. 2001; 38:192–246. [PubMed: 11750933]
71. Sterniczuk R, Dyck RH, Laferla FM, Antle MC. Characterization of the 3xTg-AD mouse model of Alzheimer's disease: part 1. Circadian changes. Brain Res. 2010; 1348:139–148. [PubMed: 20471965]
72. Pietropaolo S, Feldon J, Yee BK. Age-dependent phenotypic characteristics of a triple transgenic mouse model of Alzheimer disease. Behav Neurosci. 2008; 122:733–747. [PubMed: 18729626]
73. Carroll JC, Rosario ER, Kreimer S, Villamagna A, Gentzschein E, Stanczyk FZ, Pike CJ. Sex differences in beta-amyloid accumulation in 3xTg-AD mice: role of neonatal sex steroid hormone exposure. Brain Res. 2010; 1366:233–245. [PubMed: 20934413]

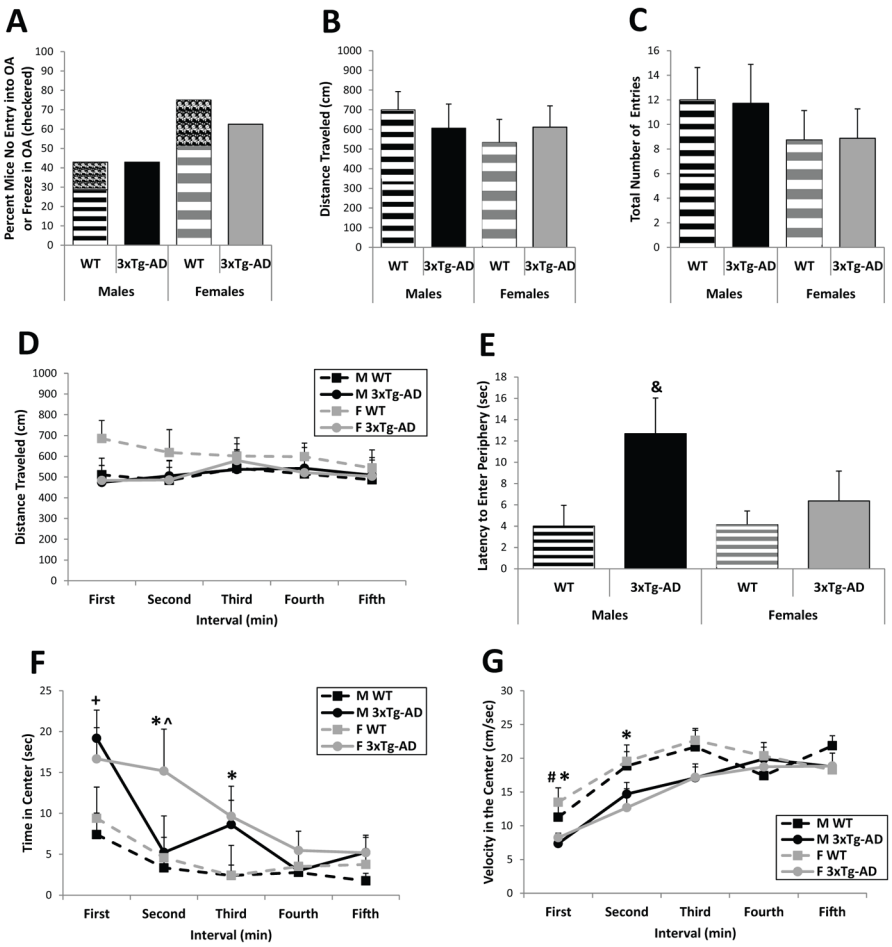

Figure 1.

EPM and open field behavior in six-month-old WT and 3xTg-AD mice. (A) Nearly half the males and more than half the females of both genotypes never entered the open arms of the EPM or they froze when they did enter an open arm (WT mice only; see checkered areas). (B and C) The distance traveled (B) and the total number of entries (C) in the EPM did not differ between 3xTg-AD and WT mice. (D) The distance traveled in the open field was also similar for 3xTg-AD and WT mice. (E) Male 3xTg-AD mice took significantly longer to enter the periphery after initial placement in the center than WT mice. (F and G) Male and female 3xTg-AD mice spent more time in the center of the open field (F) and exhibited a slower speed of movement (G) during the early part of the test (but they did not freeze—see Latency to Move in Table 1). Data represent mean ± SEM. $^{\&}p<0.05$ vs. WT mice, *$p<0.05$: female 3xTg-AD vs. female WT; $^{+}p=0.01$: male 3xTg-AD vs. male WT; ^$p<0.05$: female 3xTg-AD vs. male 3xTg-AD; $^{\#}p<0.05$: male 3xTg-AD vs. female WT.

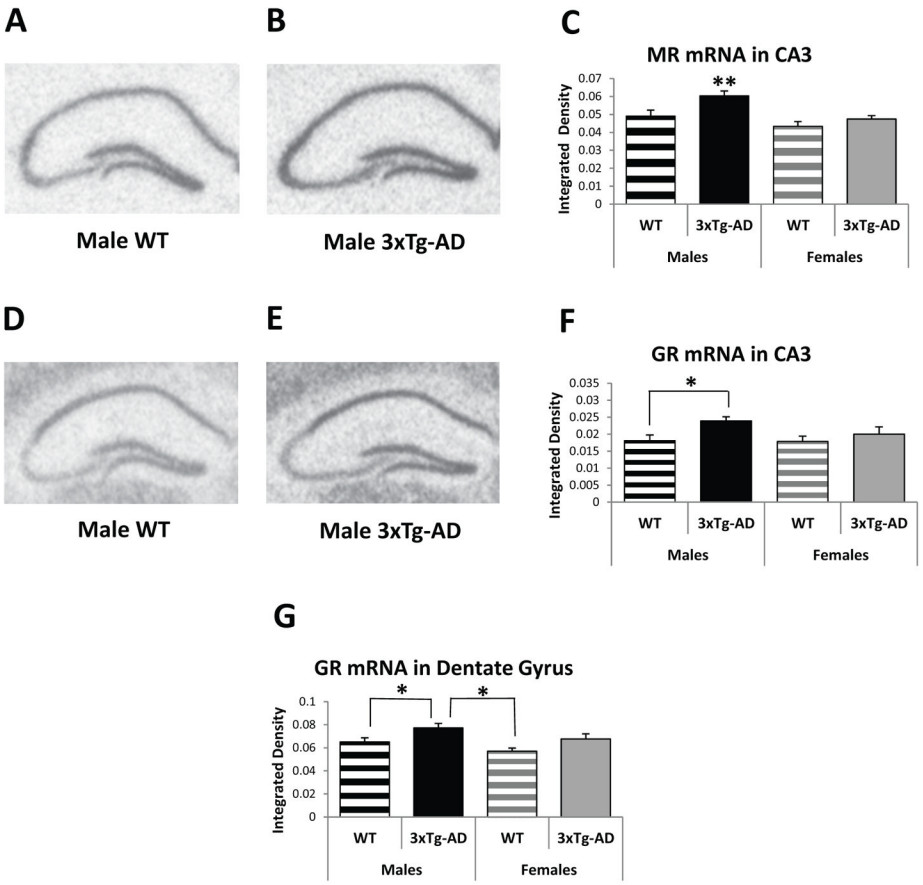

Figure 2.

Basal Gene Expression in the hippocampus (HPC) of 3–4-month-old WT and 3xTg-AD mice. (A and B) Representative MR *in situ* hybridization autoradiographs from male WT (A) and 3xTg-AD (B) mice. (C) Male 3xTg-AD mice show higher MR mRNA expression in the CA3 area of the HPC compared to male WT mice and all female mice. (D and E) Representative GR *in situ* hybridization autoradiographs of the HPC from male WT (D) and 3xTg-AD (E) mice. (F and G) Male 3xTg-AD mice exhibit higher GR mRNA expression in the CA3 area (F) and dentate gyrus (G) of the HPC compared to male WT mice and female and male WT mice, respectively. Data represent mean ± SEM. *p<0.05; **p<0.01.

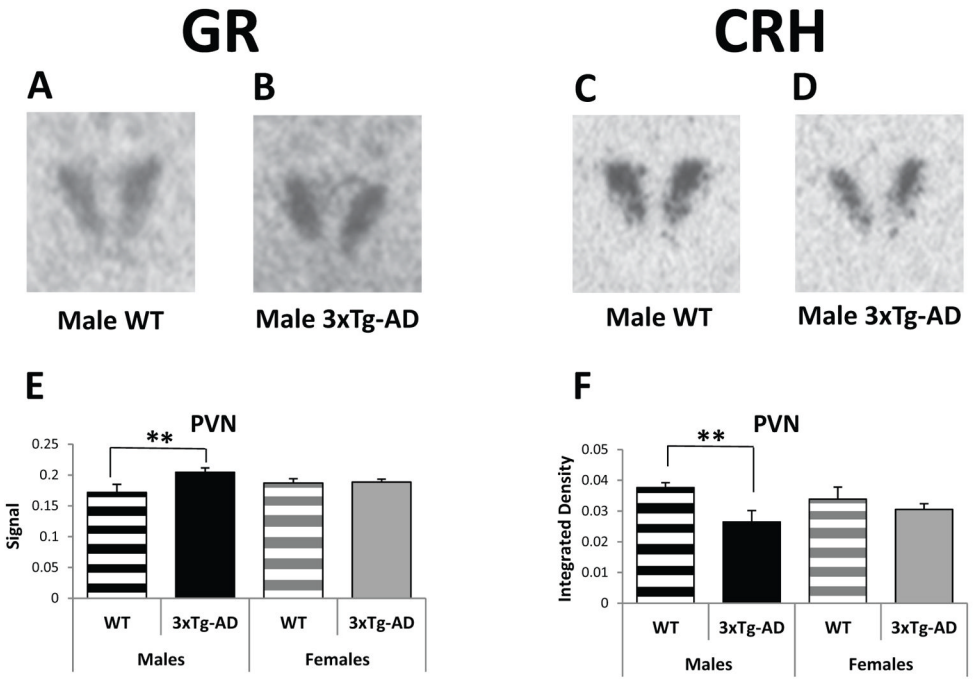

Figure 3.

Basal Gene Expression in the paraventricular nucleus of the hypothalamus (PVN) of 3–4-month-old WT and 3xTg-AD mice. (A and B) Representative GR *in situ* hybridization autoradiographs of the PVN from male WT (A) and 3xTg-AD (B) mice. (C and D) Representative CRH *in situ* hybridization autoradiographs of the PVN from male WT (C) and 3xTg-AD (D) mice. (E) Male 3xTg-AD mice show higher GR mRNA expression in the PVN than male WT mice. (F) Male 3xTg-AD mice exhibit lower CRH mRNA levels in the PVN compared to male WT mice. Data represent mean ± SEM. **p<0.01.

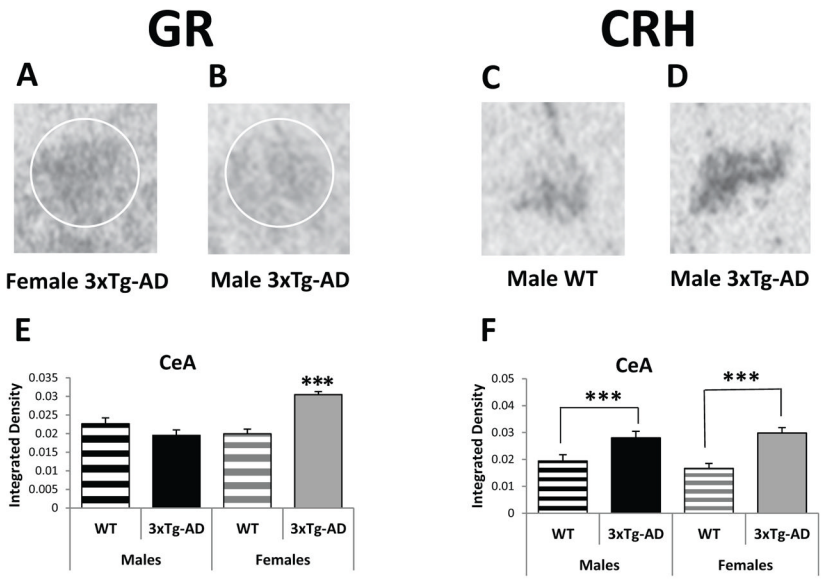

Figure 4.

Basal Gene Expression in the central nucleus of the amygdala (CeA) of 3–4-month-old WT and 3xTg-AD mice. (A and B) Representative GR *in situ* hybridization autoradiographs of the CeA from female (A) and male (B) 3xTg-AD mice. (C and D) Representative CRH *in situ* hybridization autoradiographs of the CeA from male WT (C) and male 3xTg-AD (D) mice. (E) Female 3xTg-AD mice express higher GR mRNA levels in the CeA than male 3xTg-AD mice and all WT mice. (F) All transgenic mice exhibit higher CRH mRNA expression in the CeA compared to WT mice. Data represent mean ± SEM. ***$p<0.001$.

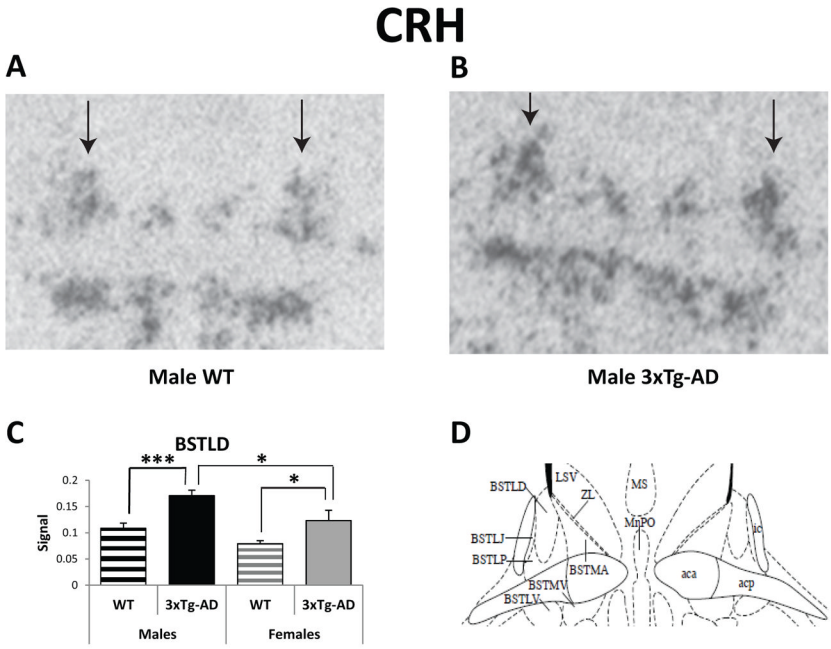

Figure 5.

Basal CRH Gene Expression in the dorsolateral bed nucleus of the stria terminalis (BSTLD) of 3-4-month-old WT and 3xTg-AD mice. (A and B) Representative CRH *in situ* hybridization autoradiographs of the BSTLD from male WT (A) and 3xTg-AD (B) mice. Arrows indicate the dorsolateral division of BST. (C) All transgenic mice exhibit higher CRH mRNA expression in the BSTLD compared to WT mice. (D) Schematic of BST nuclei, including the dorsolateral division [44]. Data represent mean ± SEM. *p<0.05; ***p<0.001.

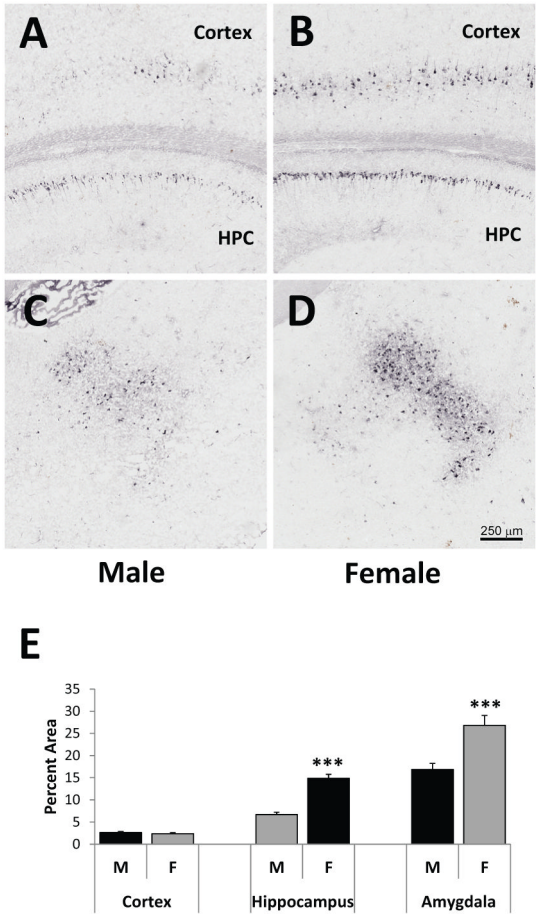

Figure 6.

hAβPP/Aβ immunoreactivity in the hippocampus (HPC), posterior parietal association cortex, and posterior basolateral amygdala of 3-month-old male and female 3xTg-AD mice. Representative images of 6E10 immunoreactivity in brain slices at Bregma −2.18 [44] of male (A and C) and female (B and D) 3xTg-AD mice are depicted here. 6E10 immunoreactivity is found in the pyramidal cell layer of the CA1–CA3 areas of the HPC, with little to no staining of fibers in the stratum radiatum or oriens. 6E10 immunoreactivity is also found in Layers IV and V of the cortex and the basolateral amygdala. No 6E10-immunopositive plaques were found. Females exhibit significantly more 6E10 immunoreactivity per area (as measured by percent area sampled) than males in the CA1 area of the HPC and the basolateral amygdala, but not the posterior parietal association cortex. ***$p<0.001$.

Table 1

Measures of Emotionality in 6-month-old 3xTg-AD mice

	Male		Female	
	WT	**3xTg-AD**	**WT**	**3xTg-AD**
Latency to Move (sec)				
EPM	0.81±0.43	4.67±2.14**	0.71±0.47	5.07±1.57**
Open Field	0.65±0.26	2.41±1.09	1.25±0.69	0.69±0.47
Defecation Boli (number)				
EPM	2.86±0.63	4.86±0.55*	3.63±0.53	4.00±0.60
Open Field	2.57±0.53	5.00±0.44*	3.63±0.86	4.75±0.53

Measures related to emotionality in the EPM and open field tests are shown here. Results are mean ± SEM. Initial freezing behavior was observed in male and female 3xTg-AD mice immediately after being placed in the EPM, but not the open field. Increased defecation was observed in male but not female 3xTg-AD mice compared to WT mice in the EPM and open field.

* $p<0.05$,

** $p<0.01$.

Table 2

Basal CORT levels in 3xTg-AD mice

		3–4 Months Old	6 Months Old
Males	WT	1.39 ± 0.59	0.79±0.44
	3xTg-AD	1.26 ± 0.56	2.06±0.99
Females	WT	4.34 ± 0.99 *	5.87±2.22 *
	3xTg-AD	6.18 ± 2.12 *	2.53±1.06

Basal CORT levels (μg/dl) were obtained from mice killed within 2 minutes after removal from their home cages between 7 and 10 A.M. No differences in CORT levels were found between WT and 3xTg-AD mice at 3–4 months of age. Females exhibited significantly higher CORT levels than males at this age. At 6 months of age, female WT mice exhibited higher CORT levels than all other mice, but note the high variability in CORT levels in the female WT mice.

* $p<0.05$.